DETERMINATION OF THE TEMPERATURE AND STRESS DEPENDENCY OF POROUS CONTINUOUS FIBER-REINFORCED COMPOSITE MATERIALS PERMEABILITY THROUGH EXPERIEMENT AND SIMULATION

Wissam BOUAJILA[(1)], Jörg RICCIUS[(1)]

[(1)] German Aerospace Centre – DLR Lampoldshausen, Langer Grund, D-74239 Hardthausen (Germany), Email: wissam.bouajila@dlr.de; joerg.riccius@dlr.de

KEYWORDS: composite materials, ceramic matrix, transpiration cooling, effusion cooling, permeability determination, temperature dependency, stress dependency.

ABSTRACT:

In the framework of the ATLLAS project co-funded by the European Commission within the 7th Framework Programme, ceramic matrix composites were investigated as candidate materials for transpiration cooled combustor walls of ramjets. The permeability of C/C random (±15° standard quality) and OXIPOL (3x pyrolysed, 0|90° standard quality) has been measured at ambient and elevated temperatures using stress-free and stressed samples at DLR Lampoldshausen.

The permeability of the material was defined using 2 parameters, the intrinsic (Darcy´s) permeability *K* and the Forchheimer´s permeability *G*.

For a stress-free sample, it has been observed that an increase in temperature of 20% relative to ambient resulted in a reduction of the permeability coefficients. For C/C random perpendicular, the reduction in the coefficient values is about - 32 % for *K* and - 2 % for *G*. For OXIPOL 3x pyrolysed, it is about - 34 % for *K* and - 18 % for *G*.

The comparison of the measurements from the tests performed at ambient temperature with a stress-free sample and a stressed sample showed that the permeability coefficients seemed to steadily decrease with increasing the compression stress of the test sample. For C/C random parallel, an estimated average compression stress of about 70 MPa resulted in a drop of about 29 % of *K* and *G* at 298 K.

1 INTRODUCTION

The project ATLLAS (Aero-Thermodynamic Loads on Lightweight Advanced Structures) funded by the European Commission within the 7h European Framework Programme evaluated several lightweight materials which can withstand the extreme temperatures and high heat fluxes typical for high-speed flights above Mach 3 [1]. At these speeds, classical materials used for airframes and propulsion units are no longer qualified and need to be replaced by high-temperature resistant, lightweight materials, with active cooling of some parts.
Materials and cooling techniques and their interaction with the aero-thermal loads were addressed in ATLLAS for both the airframe and propulsion components such as combustion chamber liners coping with different aero-thermal loads.
The thermally highly loaded walls of the propulsion units require particular material development. CMC (Ceramic Matrix Composites)-based combustors with effusion cooled walls were shown to have a great potential as lightweight material combined with active cooling such as effusion cooling [1].
The effusion cooling concept is widely used as cooling method of inner liners of gas turbine combustors [2]. Over the last few years, DLR has been working on the development of effusion cooling designs to be used for the cooling of rocket engine thrust chambers. Investigations performed by DLR Lampoldshausen have demonstrated the capability of effusion cooled carbon fiber / carbon matrix (C/C) composite materials to well perform as a thrust chamber liner material [3] [4] [5] [6] [7]: low specific weight, high specific strength and very low thermal expansion over a large temperature range.

To comply with the specifications defined for the ATLLAS ramjet concept, the combustion of the fuel has to be carried out at a high pressure in the combustor. These combustion conditions would release a large quantity of heat that has to be

managed in order to keep the wall material below a critical temperature to prevent damage of the combustor wall in service. Although the combustor wall would be actively cooled by the fuel through effusion cooling, the efficiency of effusion cooling is dependent on the permeability of the wall material which is an intrinsic quantity that is independent of the fluid.

While the permeability of porous materials is commonly assumed to be an intrinsic quantity that is independent of the test/service conditions e.g. temperature and stress state of the porous material [5], the present work focused on investigating the validity of such an assumption. Tests with samples made of C/C random (±15° standard quality) and OXIPOL (3x pyrolysed, 0|90° standard quality) and using GH2 and GN2 as fluid have been carried out at different temperatures over a wide range of fluid pressure to assess the influence of temperature and stress state of the porous medium on its permeability. The results of this investigation are summarized in the present paper.

2 ATLLAS TEST SAMPLE AND DLR TEST BENCH

A test campaign has been carried out at DLR Lampoldshausen to measure the permeability of various ATLLAS test samples. Among the two measurement methods commonly used to measure the permeability of porous materials, the transitory method [8], and the stationary method [9], the stationary method is considered in this work.

2.1 ATLLAS test samples

The structure of the ATLLAS CMC bulk material consists of a stack of sheets of plain weave fabric in layers that have been thermally cured under pressure [10]. Two CMC materials have been tested during the ATLLAS test campaign at DLR Lampoldshausen: C/C random (±15° standard quality) and OXIPOL (3x pyrolysed, 0|90° standard quality).

2.1.1 Test sample geometry

As illustrated in Figure 1, 30 mm long slightly conical test samples have been used in the tests performed at the DLR Lampoldshausen. While the inlet diameter is 31 mm, the outlet diameter is slightly reduced to 30 mm. This slightly conical shape has been preferred to a cylindrical shape to firstly, enhance the sealing of the test sample and secondly, to prevent the sample from being dragged downstream by the fluid flow.

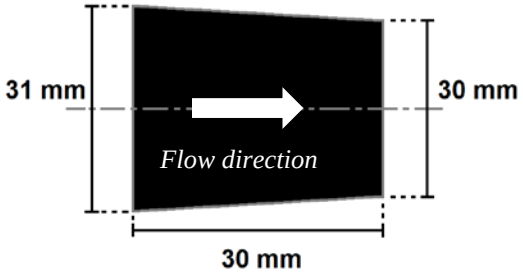

Figure 1. Drawing of the ATLLAS test sample geometry (with magnified angles)

2.1.2 Test sample configurations

For both, C/C random and OXIPOL, two configurations of the test samples have been considered: “parallel” samples and “perpendicular” ones. A sample is referred to as “parallel” when the direction of the fluid flow is parallel to the sheets of the plain weave fabric and as “perpendicular” when the fluid flows in a perpendicular direction to the sheets of the plain weave fabric. The samples tested with GN2 and GH2 at P6.1 are summarized in Table 1 below:

	C/C random	OXIPOL
Parallel	PH1431-03[b]	I678-L-03[a]
Perpendicular	PH1431-02[a]	

[a] used to investigate the dependency of permeability on temperature
[b] used to investigate the dependency of permeability on stress

Table 1. ATLLAS CMC test sample configurations

2.2 DLR Lampoldshausen test bench P6.1

2.2.1 Experimental set up

The experimental set up used for the measurement of the permeability of the porous material samples at the DLR Lampoldshausen test facility P6.1 is shown in Figure 2. Two valves (one at the fluid inlet and the other at the fluid outlet) enable to control the inlet and the outlet fluid pressure. The mass flow rate is measured using a Coriolis flow meter CFM010. Both, the inlet pressure and the outlet pressure are measured using pressure sensors HBM P3MA. The pressure drop along the sample is measured using a differential pressure sensor Althen AD122MK to ensure a good accuracy of the measurements. Thermocouples Type K Class 1 are used for the measurement of the fluid temperature and the sample temperature.

The heating of the sample is achieved by heating the sample holder made of copper using flexible heaters as shown in Figure 13.

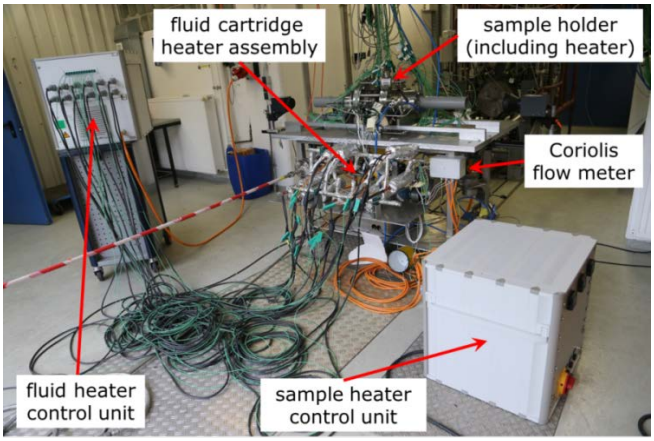

Figure 2. Permeability measurement test set up at DLR Lampoldshausen test facility P6.1

2.2.2 Measurement accuracy

The characteristics and the accuracy of the measurement devices of the permeability measurement test set up at DLR Lampoldshausen test bench P6.1 are summarized in the following Table 2.

	Device	**Measuring range**	**Accuracy, linearity and repeatability**
Pressure	HBM P3MA	100 bar	0.4 % [11]
Pressure difference	Althen AD122MK	±50 bar	0.45 % [12]
Mass flow rate	Micro Motion Elite CMF010M	93.5 kg/h (nominal) 108 kg/h (maximal)	0.35 % [a] [13] (on gases)
Temperature	Thermocouple type K class 1	-40 °C to 375 °C	0.5 °C [14]

[a] for a mass flow rate below 5% of the nominal mass flow meter, the accuracy of the measured mass flow rate is defined as: Accuracy (%) = zero stability / mass flow rate * 100 where zero stability = 0.002 kg/h for CMF010M[1]

Table 2. Characteristics and accuracy of the measurement devices of the permeability measurement test set up at DLR Lampoldshausen test facility P6.1

3 MODELING OF ATLLAS TEST SAMPLE MATERIAL PERMEABILTY

Assuming the fluid is flowing through the C/C material in a transitory regime (neither laminar nor turbulent), e.g. 10 < Re < 1000, the pressure loss along the sample can be predicted using the Forchheimer´s model, which can be seen as a combination of the Darcy´s law and the Burke-Plummer´s model

$$-\frac{\partial P}{\partial x} = \frac{\mu}{K}U + \frac{\rho}{G}\|U\|U \qquad (1)$$

where μ and ρ is the dynamic viscosity of the fluid and the density of the fluid, respectively; K and G is the intrinsic permeability and the Forchheimer coefficient of the porous medium, respectively.

Assuming as if the fluid was the only phase present in the porous medium, the superficial velocity of the fluid U is related to the mass flow $\dot{m}$ through

$$U = \frac{\dot{m}}{\rho A} \qquad (2)$$

with A, the area of the entire surface normal to the direction of the flow. For the cylindrical sample with a diameter D, the area of the surface normal to the flow is

$$A = \pi\frac{D^2}{4} \qquad (3)$$

Substituting (2) and (3) in (1), the pressure gradient $(\partial P/\partial x)_i$ for a portion i of the cylindrical test probe can be approximated as

$$\left(\frac{\partial P}{\partial x}\right)_i \cong \frac{\Delta P_i}{\Delta x} = \frac{\mu}{K}\frac{\dot{m}}{\rho_i A} + \frac{\rho_i}{G}\left(\frac{\dot{m}}{\rho_i A}\right)^2 \qquad (4)$$

where ΔP_i is the pressure difference in the portion i and defined as

$$\Delta P_i = P_i - P_{i+1} \qquad (5)$$

with P_i, and P_{i+1}, the inlet flow pressure and the outlet flow pressure for the portion i, respectively. The mass flow $\dot{m}$ is constant along the cylindrical test probe.

1 URL://http://www2.emersonprocess.com/siteadmincenter/PM%20Micro%20Motion%20Documents/ELITE-PDS-PS-00374.pdf (visited on 19.12.2014)

4 DEPENDENCY OF THE ATLLAS TEST SAMPLE PERMEABILITY ON TEMPERATURE

4.1 Test campaign

A set of three tests using GN2 at a pressure of 40 bar as permeability test fluid has been performed with every ATLLAS test sample C/C random perpendicular and OXIPOL parallel. Different temperatures for both the fluid and the sample have been defined as shown in Table 3. The first test has been carried out at room temperature whereas the two following tests have been performed at higher temperatures.

Test	Fluid	Fluid pressure	Fluid heating	Sample heating
A-*i*	GN2	40 bar	Ambient	Ambient
B-*i*	GN2	40 bar	150°C	100°C
C-*i*	GN2	40 bar	215°C	100°C

Table 3. Set of 3 tests performed with every ATLLAS test sample; i=1 for C/C random perpendicular and i=2 for OXIPOL parallel

4.2 Test data processing

To determine the permeability coefficients of the test sample material at elevated temperature, an interpolation of the experimental data of the two tests carried out at elevated temperature (B-*i* and C-*i* in Table 3) has to be done. The purpose of the interpolation procedure is to emulate an isothermal case at elevated temperature by assuming a same temperature for the test sample and the permeability test fluid. By doing so, a unique temperature for both the sample and the fluid is obtained, as it is for the test at ambient temperature (A-*i* in Table 3). The only requirement to fulfill for the interpolation procedure is that the temperature of the sample is not too different for the two considered elevated temperature tests, which is the case in this work. More details can be found in [15].

4.3 Results and discussion

4.3.1 Assumption and methodologies for the definition of the permeability parameters

Two approaches have been used to process the experimental data and determine the permeability parameters of an ATLLAS test sample:

1. Constant parameter ratio *Q*: although the material permeability parameters (*K*, *G*) are assumed to be temperature dependent, the parameter ratio *Q* (=*K*/*G*) is here assumed to be independent of temperature. The value of the ratio *Q* is the same for the test at ambient temperature and the test at "isothermal" elevated temperature (interpolated data). In this parameter determination approach, the three parameters (K_{RT}, K_{isoET}, *Q*) are determined fitting the two sets of data (ambient temperature data set and "isothermal" elevated temperature data set) simultaneously. More information is available in [15].
2. Variable parameter ratio *Q*: no assumption made regarding the value of the ratio *Q*. The value of *Q* might be different for the test at ambient temperature and the test at "isothermal" elevated temperature (interpolated data). The set of permeability parameters (*K*, *G*) is determined fitting every set of data (ambient temperature data set or "isothermal" elevated temperature data set) separately.

4.3.2 Dependency of the permeability on temperature for C/C random perpendicular

The values of the permeability parameters are determined by fitting the experimental data. As illustrated in Figure 3, the fit shows a good agreement with the experimental data over the considered mass flow rate range for the two temperatures. This result highlights the good accuracy of the optimized values of the permeability coefficients.

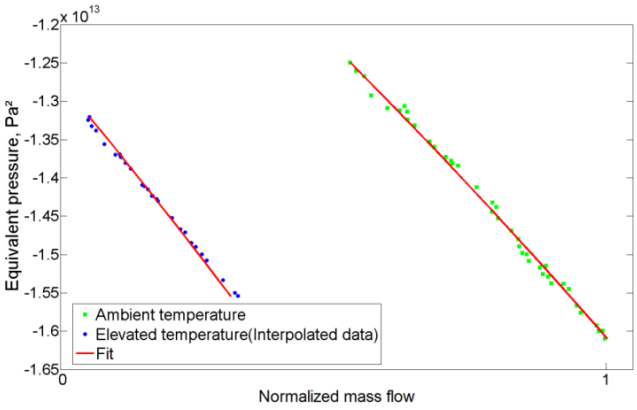

Figure 3. Fit of the experimental data for the ATLLAS test sample C/C random perpendicular

The values of Darcy´s permeability *K* from both permeability parameter determination approaches (variable ratio *Q* and constant ratio *Q*) are compared in Figure 4 for stress-free C/C random perpendicular. The values from both permeability parameter determination approaches are close although there is a larger scattering at 300 K than at 360 K. The fit of the defined *K* values shows a significant reduction of *K* when temperature increases.

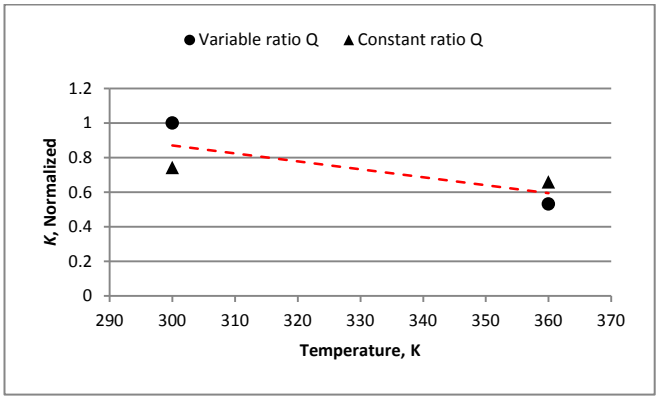

Figure 4. Evolution of the permeability parameter K (Darcy´s permeability) with temperature for stress-free C/C random perpendicular

The values of Forchheimer´s permeability *G* from both permeability parameter determination approaches (variable ratio *Q* and constant ratio *Q*) are compared in Figure 5 for stress-free C/C random perpendicular. The values from both permeability parameter determination approaches are quite close. The fit of the values shows a slight reduction of *G* when temperature increases.

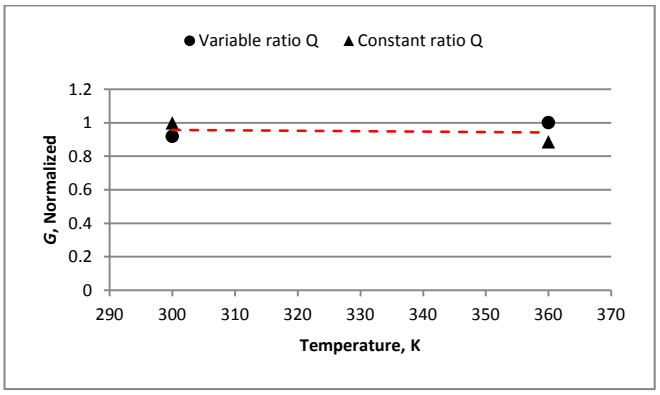

Figure 5. Evolution of the permeability parameter G (Forchheimer´s permeability) with temperature for stress-free C/C random perpendicular

Average values of the parameters *K* and *G* are considered to investigate the extent of the temperature influence on the permeability parameters values. The change in the average value of the permeability parameters of C/C random perpendicular at 360 K relative to its values at ambient temperature is shown in Table 4. According to the obtained results, an increase in temperature of 20% relative to ambient temperature results in a strong decrease of the Darcy´s permeability *K* (-32%) while the Forchheimer´s permeability *G* slightly decreases (-2%). One can then notice that an increase in temperature seems to result in a decrease of the value of the permeability parameters. For C/C random perpendicular, the parameter *K* seems to be more sensitive than the parameter *G* to temperature change.

Sample	*T*ref (K)	*T* (K)	Δ*K* (%)	Δ*G* (%)
CC Random Perpendicular	300	360	-32	-2

Table 4. Change in the permeability parameter of stress-free C/C random perpendicular at 360 K relative to its values at 300 K

4.3.3 Dependency of the permeability on temperature for OXIPOL parallel

As for C/C random perpendicular case, the values of the permeability parameters are determined by fitting the experimental data. As illustrated in Figure 6, the fit shows a good agreement with the experimental data over the considered mass flow rate range for the two temperatures. This result highlights the good accuracy of the optimized values of the coefficients.

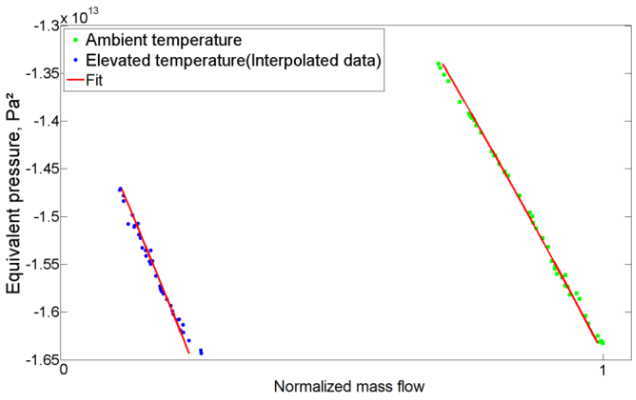

Figure 6. Fit of the experimental data for the ATLLAS test sample OXIPOL parallel

The values of Darcy´s permeability *K* from both permeability parameter determination approaches (variable ratio *Q* and constant ratio *Q*) are compared in Figure 7 for stress-free OXIPOL parallel. The values from both permeability parameter determination approaches are quite close despite some scattering is observed at 360 K. The fit of the defined *K* values shows a significant reduction of *K* when temperature increases.

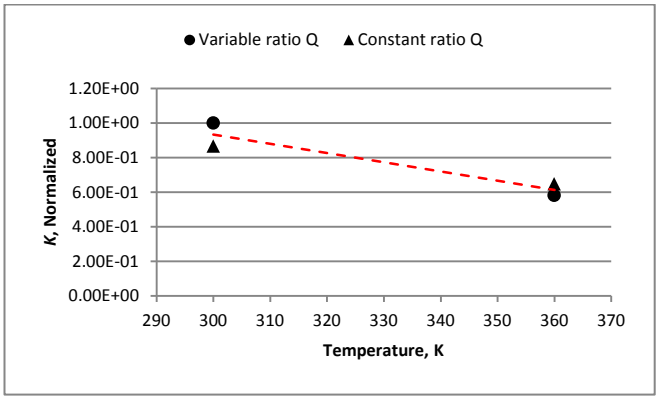

Figure 7. Evolution of the permeability parameter K (Darcy´s permeability) with temperature for stress-free OXIPOL parallel

The values of Forchheimer´s permeability *G* from both permeability parameter determination approaches (variable ratio *Q* and constant ratio *Q*) are compared in Figure 8 for stress-free OXIPOL parallel. The values from both permeability parameter determination approaches are almost similar at 300K and at 360K. Unlike C/C random perpendicular, the fit of the values of *G* shows a significant reduction of the parameter when temperature increases for OXIPOL parallel.

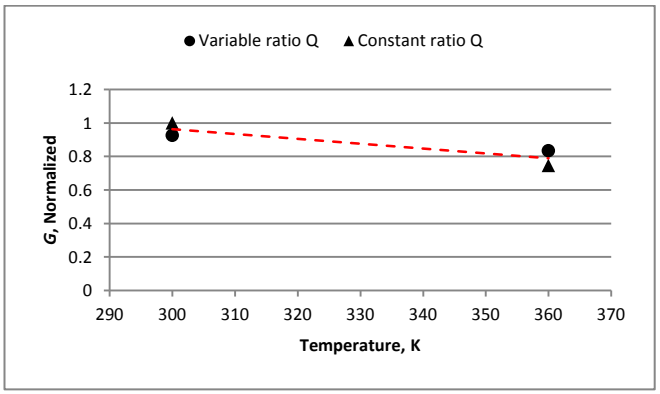

Figure 8. Evolution of the permeability parameter G (Forchheimer´s permeability) with temperature for stress-free OXIPOL parallel

As for C/C random perpendicular, average values of the parameters *K* and *G* are considered to investigate the extent of the temperature influence on the permeability parameters values. The change in the average value of the permeability parameters of OXIPOL parallel, when temperature increases from ambient to 360 K, is shown in Table 5 below. According to the obtained results, an increase in temperature of 20% relative to ambient temperature results in a strong decrease of both the Darcy´s permeability *K* (-32%) and the Forchheimer´s permeability *G* (-18%). As for C/C random perpendicular, one can notice that an increase in temperature seems to result in a decrease of the value of the permeability parameters for OXIPOL parallel. As for C/C random perpendicular, the parameter *K* seems to be more sensitive than the parameter *G* to temperature change.

Sample	***T*ref (K)**	***T* (K)**	**Δ*K* (%)**	**Δ*G* (%)**
CC Random Perpendicular	300	360	-34	-18

Table 5. Change in the permeability parameter of stress-free OXIPOL parallel at 360 K relative to its values at 300 K

5 EVOLUTION OF THE PERMEABILITY PARAMETERS AS A FUNCTION OF THE SAMPLE STRESS STATE

For the investigation of the dependency of permeability on the stress state of the test sample, only a single ATLLAS test sample (C/C random parallel) has been tested. The permeability parameter values reported in the following are all at 283 K.

5.1 Test campaign

Three tests have been performed to assess the influence of the stress state of the test sample on its permeability. Only a single test sample C/C random parallel has been used during this test campaign. The test sample has not been removed from the sample holder in between these three tests.

5.1.1 Principle of the test

A run of three consecutive thermal loads is defined for each test. For each test, it was planned to perform a run at elevated temperature, preceded and followed by a run at ambient temperature, as illustrated in Figure 9. Before the first elevated temperature run, the test sample is assumed stress free (at run A). During the elevated temperature run (run B) and due to the difference in the thermal expansion of the sample holder made of copper and of the test sample made of carbon, the sample holder will expand more than the test sample does, releasing the test sample which will be dragged downstream by the flow and hold by the sample holder in a new position. During the cooling down phase, the sample holder will contract around the test sample back to its initial size and it will tighten the sample. This thermal expansion difference-induced tightening of the sample will result in a new stress state of the test sample for the following run at ambient temperature (run C). According to this test procedure, two stress states of the test sample at room temperature are obtained per test.

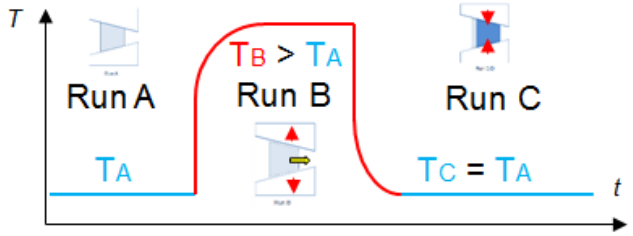

Figure 9. Illustration of the temperature load path defined for each of the three tests with the resulting thermal expansion/contraction of the sample holder and the downstream drag of the sample

5.1.2 Performed tests

Three permeability measurement tests with a unique ATLLAS test sample C/C random parallel have been performed. GH2 at a pressure of 40 bars has been used as test fluid. For each of the three tests, three sequences of temperature without interruption have been defined. The test sample has not been removed from the sample holder at the end of each of these tests. The test conditions of the three tests are summarized in Table 6. Although the elevated temperature sequence has to be followed by a test sequence at room temperature for each test, the heater was left switched on unintentionally during the last sequence of the last two tests (2 and 3) resulting in an elevated temperature in the third sequence as reported in Table 6. In the following, the temperature of 283 K (in run A, C, D, and F) will be referred to as ambient temperature.

Test	**1**			**2**			**3**		
Run	A	B	C	D	E1	E2	F	G1	G2
Fluid	GH2			GH2			GH2		
P_{fluid} (bar)	40			40			40		
T_{fluid} (°C)	10	92	10	12	105	105	12	147	147
T_{sample} (°C)	10	100	20	11	167	167	11	174	174
Stress state	0	0	σ_1	σ_1	0	0	σ_2	0	0

Table 6. Test conditions and expected stress state of the test sample

5.2 Determination of the permeability parameters

5.2.1 Processing of the experimental data

Three permeability tests have been carried out to investigate the influence of the stress state of the sample on its permeability. According to the defined testing procedure, the test sample has not been removed from the sample holder at the end of each of the three tests. The following test started with the test sample in the position and state where it was left at the end of the previous test. The comparison in Figure 10 of the experimental data from the last sequence of the first test (run C) to those from the first sequence of the following test (run D) shows that the data are quite similar. These results shows that the state of the test sample can be assumed unchanged between two successive permeability tests.

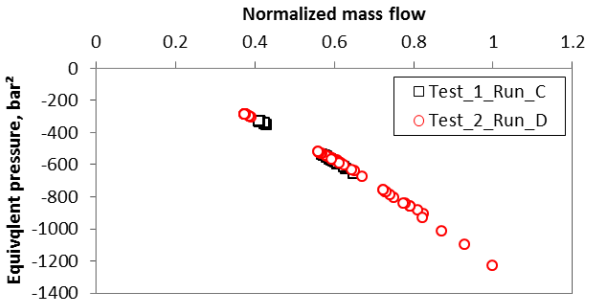

Figure 10. Comparison of the experimental data from the last sequence of test 1 (run C) and the first sequence of test 2 (run D)

Based on the previous observation, that the test sample can be assumed unchanged between two successive permeability tests, the three performed permeability tests 1, 2, and 3 can then be regarded as being performed without interruption. A drawing of the resulting temperature load path is shown in Figure 11.

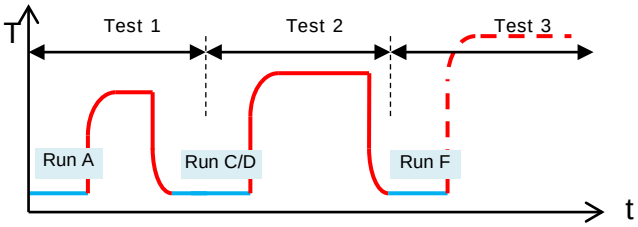

Figure 11. Illustration of the temperature load with regarding the three permeability tests 1, 2, and 3 as being performed without interruption

As illustrated using blue-color lines in Figure 11 above, only the data from the sequences at ambient temperature (run A, run C/D, and run F) are considered for the assessment of the dependency of the permeability on the stress state of the ATLLAS test sample at ambient temperature in the present work.

5.2.2 Parameter determination approaches

As in the investigation of the temperature dependency of the permeability parameters, two approaches have been used to process the experimental data and determine the permeability parameters of an ATLLAS test sample as a function of its stress state:

1. Constant parameter ratio *Q*: the parameter ratio *Q* (=*K*/*G*) is assumed to be not dependent on the stress state of the test sample. The value of *Q* is the same for a test with a stress-free test sample and for a

test with a stressed test sample. Considering three tests, three values of K and then a common value of Q have to be determined [15]. The permeability parameters to be defined are K_{run_A}, $K_{run\_C/D}$, K_{run_F}, and Q. These four permeability parameters are determined simultaneously using all data at ambient temperature from the three tests. These permeability parameters are determined by fitting the experimental measurement according to the least-squares fit method.

2. Variable parameter ratio Q: no assumption made regarding the value of Q. The value of Q will be different for a test with a stress-free test sample and for a test with a stressed test sample. The set of permeability parameters (K, G) is determined fitting every set of data (data from either run A or run CD or run F) separately. The fit of the experimental measurement is performed according to the least-squares fit method.

5.2.3 Permeability parameters values:

The fit of the experimental data from the room temperature sequences from the three permeability test is shown in the following Figure 12. The fit of the data is within the scattering of the measurement and shows a good agreement with the experiment. The values of the fitted permeability parameters can therefore be assumed as accurate. From the plot in Figure 12, one can see that the more the sample is compressed, the more the mass flow is reduced for a given equivalent pressure of the fluid. This is a first evidence that the permeability of a porous material can be dependent on the stress state of the material.

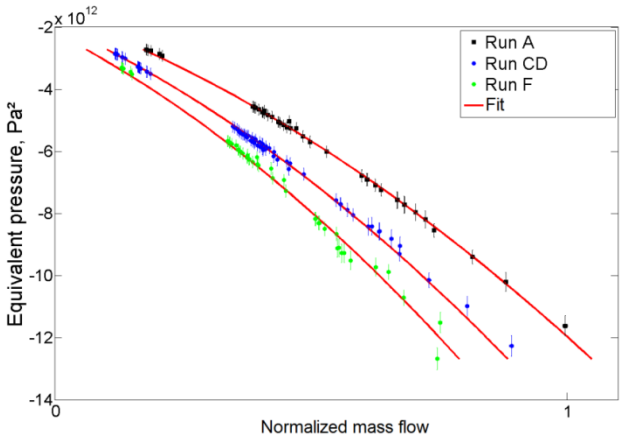

Figure 12. Fit of the experimental data of the room temperature sequences from the three tests

As done in the investigation of the temperature dependency of the permeability parameters, average value of K and G are calculated from the results of the two permeability parameter determination approaches. These average values of K and G will be used in the following to assess the extent of the influence of the material stress state on its permeability.

The change in the average values of the permeability parameters of the ATLLAS test sample C/C random parallel at the different stress states relative to its values at the stress-free state of the sample are summarized in Table 7. The results show that increasing the stress level of the test sample seems to result in a decrease of both the Darcy´s permeability K and the Forchheimer´s permeability G. Consequently, it can be concluded that the permeability of the test sample is sensitive to the sample stress state.

Sample	T (K)	Run	Stress level	ΔK (%)	ΔG (%)
C/C random parallel	283	A	0	0	0
		C/D	σ_1	-23	-16
		F	σ_2	-28	-29

Table 7. Permeability parameters of C/C random parallel at 283 K for three stress states of the test sample

6 ASSESSMENT OF THE INFLUENCE OF STRESS ON PERMEABILITY

6.1 First assessment of the stress level in the test sample

As the mechanical load applied by the sample holder on the test sample has not been measured during the tests, structural analyses of the permeability test bench are performed to assess the stress level in the test sample resulting from the tightening of the test sample by the sample holder at the cooling down stage following an elevated temperature run. Since the interaction of the test sample with the sample holder is of a high importance, both the test sample and the sample holder have been modeled considering contact elements.

6.1.1 Presentation of the Finite Element analyses

- *Assumptions:*

Both the test sample and the sample holder are considered for the structural Finite Element (FE) analysis. The sample holder is assumed made of copper whose properties are available in open literature [16]. The test sample is assumed made of CMC C/C random whose properties have been partially determined by DLR Stuttgart [10].

Although the C/C random material shows orthotropic properties due to its structure (stack of sheets of plain weave fabric in layers), the material is assumed isotropic since the transversal mechanical properties are not available. Therefore, only the longitudinal mechanical properties of C/C random material are considered in the analyses to get a first assessment of the stress state of the test sample.

The temperature is assumed equal and uniformly distributed in the test sample and the sample holder at the end of the elevated temperature sequence of a permeability test. The stress in the test sample is assumed to result mainly from a) the tightening pressure applied by the sample holder and b) the thermal contraction of the sample holder during cooling after an elevated temperature test sequence. No fluid pressure is assumed to be applied on the test sample faces before starting an ambient temperature test sequence.

- *Finite Element model:*

As the C/C random material and copper are assumed to show isotropic properties and the geometry of the test sample and the geometry of the sample holder are axisymmetric as shown in Figure 13, the investigated problem is assumed axisymmetric and the FE analyses are reduced to 2-D axisymmetric cases as illustrated in Figure 14.

A relatively fine mesh is defined to well assess the distribution of the stress through the test sample. Frictional contact with a friction coefficient of 0.2 has been assumed for the contact region between the test sample and the sample holder.

As the stress state of the test sample after cooling at steady state conditions has to be determined, the analyses have been restricted to steady-state structural analyses. The commercial Finite Element analysis software package Ansys R15.0 APDL has been used for these simulations.

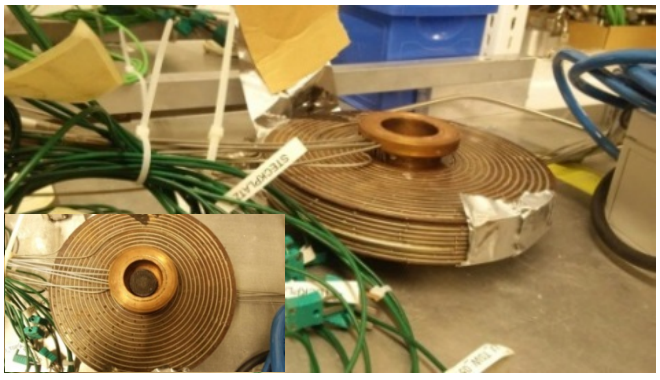

Figure 13. Pictures of the sample holder with the ATLLAS test sample left inside

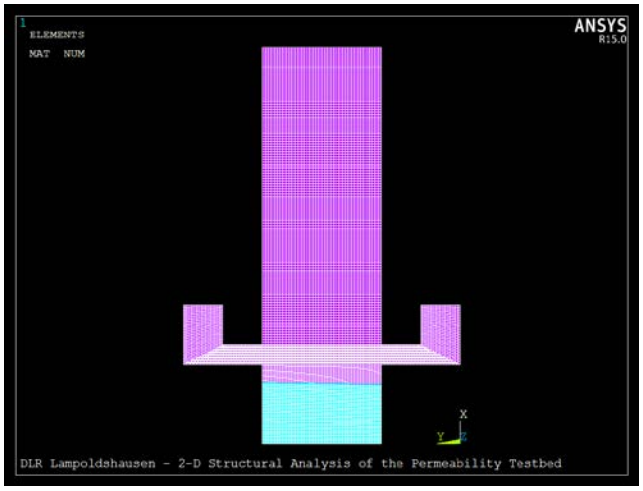

Figure 14. 2-D axisymmetric model of the sample holder and the test sample using Ansys R15.0

6.1.2 Test sample stress state and stress magnitude

The magnitude and the distribution of the stress in the test sample resulting from the thermal contraction-induced compression of the test sample by the sample holder have been determined by performing steady-state structural Finite Element analyses of the assembly sample holder/test sample. The test sample is assumed stress free during the first ambient temperature sequence of the first test (run A) as no heating has been performed before it. A Finite Element analysis has been performed for each of the 283 K sequences run C/D and run F. The temperature conditions of these simulations of the test sequences are presented in Table 8.

The magnitude and the distribution of the radial stress in the test sample for the two simulated test sequences run C/D and run F are compared in Figure 15. The larger thermal contraction of the sample holder relative to the thermal contraction of the sample induces a compression of the sample at ambient temperature. Due to the shape of the test sample (slightly conical) and the frictional contact with the sample holder, the distribution of the compressive radial stress is not uniform. The upstream sliding of the sample relative to the sample holder is negligible.

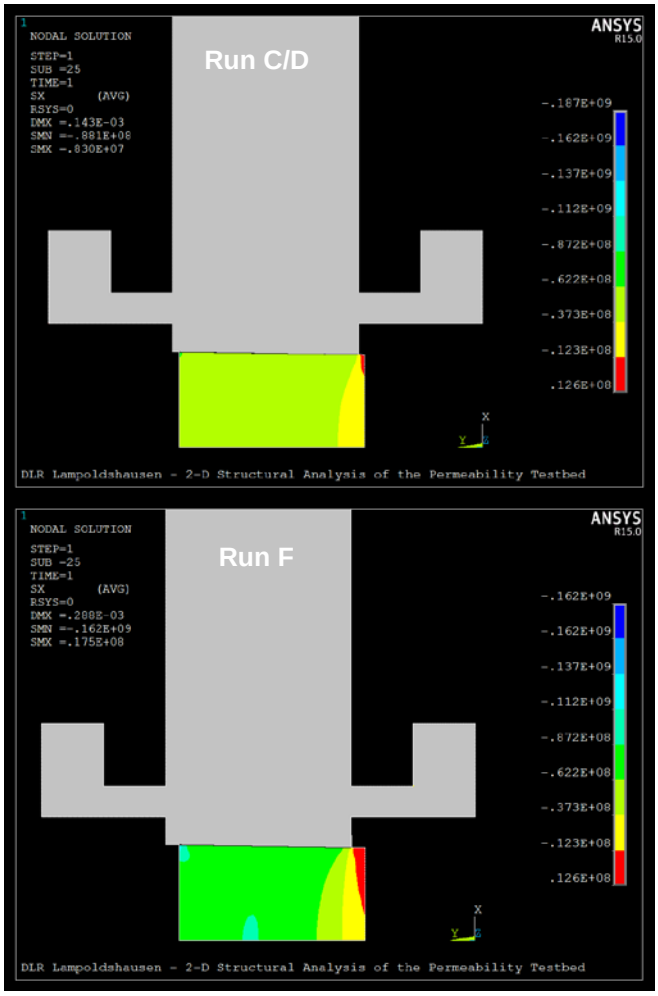

Figure 15. Magnitude and distribution of the radial stress in the test sample for run C/D and run F at 283 K (values in Pa)

The average value of the compression radial stress in the test sample is reported in Table 8 for the two test sequences run C/D and run F. The larger the temperature difference between the foregoing elevated temperature sequence and the investigated sequence, the larger the value of the average compression radial stress in the test sample. A pretest heating of the sample at a temperature of 440 K will result in an average compression stress in the test sample of about 70MPa mainly due to the thermal contraction of the sample holder at the test temperature of 283 K.

Test sample	**Test sequence**	**Initial T (K)**	**Test T (K)**	**Average radial stress (MPa)**
C/C random parallel	Run C/D	361	283	-45
	Run F	440	283	-70

Table 8. Temperature conditions of run C/D and run F and computed average radial stress in the test sample C/C random parallel

6.2 Dependency of permeability on stress for C/C random parallel

The average values of the permeability parameters of the ATLLAS test sample C/C random parallel at 283 K are compared to the calculated average radial stress values in the following Table 9. The test sample is assumed stress free during the first sequence of the first test (run A). Based on the obtained results, one can see that the larger the compression stress in the test sample, the larger the reduction of the permeability parameters.

Sample	**T (K)**	**Run**	**Stress level**	**ΔK (%)**	**ΔG (%)**
C/C random parallel	283	A	0	0	0
		C/D	-45	-23	-16
		F	-70	-28	-29

Table 9. Permeability parameters and stress levels of the ATLLAS test sample C/C random parallel at 283 K for three stress states of the test sample

The evolution of the Darcy´s permeability *K* and the Forchheimer´s permeability *G* as a function of the calculated average radial stress for the ATLLAS test sample C/C random parallel at 283 K are shown in Figure 16 and Figure 17, respectively. The results of both permeability parameters determination approaches (constant ratio *Q* and variable ratio *Q*) have been reported. One can see on these two figures that the values of the permeability parameters from the two permeability parameters determination approaches (constant ratio *Q* and variable ratio *Q*) are almost similar. Moreover, Figure 16 and Figure 17 show that the values of the permeability parameters decrease when the magnitude of the average compression radial stress increases. This result implies that the permeability of the ATLLAS test sample C/C random parallel seems to be dependent on the stress state of the test sample. The fits of the permeability parameters values highlight that the dependency of the permeability parameters of the ATLLAS test sample C/C random parallel on the average compression stress magnitude seems to be linear.

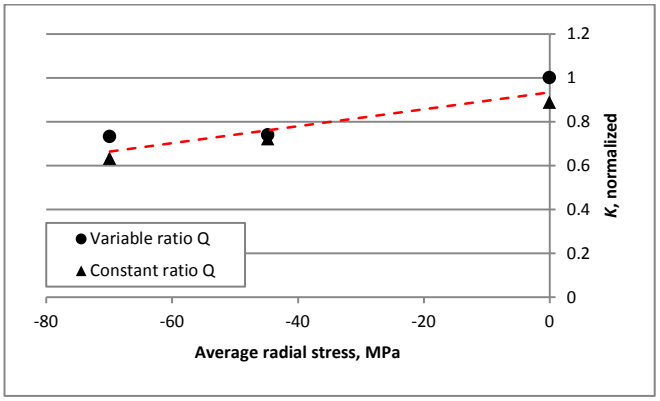

Figure 16. Evolution of the Darcy´s permeability K as a function of the average radial stress at 298 K for the ATLLAS test sample C/C random parallel

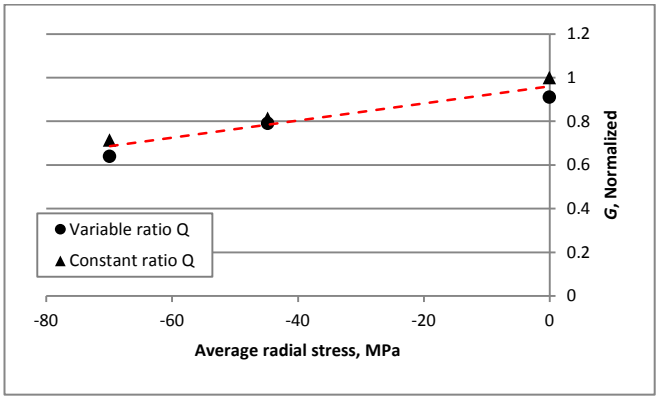

Figure 17. Evolution of the Forchheimer´s permeability G as a function of the average radial stress at 298 K for the ATLLAS test sample C/C random parallel

7 CONCLUSION AND OUTLOOK

In the framework of the ATLLAS II project, DLR Lampoldshausen has investigated the dependency of the permeability of porous materials on temperature and stress by performing various permeability tests using the DLR Lampoldshausen test bench P6.1. Approximately cylindrical ATLLAS test samples made of C/C random (±15° standard quality) and OXIPOL (3x pyrolysed, 0|90° standard quality) with two configurations (parallel and perpendicular) have been used in the test campaign. Two approaches for the determination of the permeability parameters have been compared.

The investigation of the dependency of the permeability on temperature has shown that for a stress-free sample an increase in temperature of just 60 K relative to room temperature resulted in a significant reduction of the permeability coefficients of both C/C random perpendicular and OXIPOL 3x pyrolysed parallel. This evolution of the permeability parameters implies that the permeability of a porous material is sensitive to temperature. Although the sensibility extent of the permeability on temperature seems to be dependent on the investigated porous material, a relative small increase in temperature may result in a significant reduction of the value of the permeability coefficients *K* and *G*.

The dependency of the permeability of a porous material on stress has been investigated using the ATLLAS test sample made of C/C random parallel. The comparison of the data from the test sequences obtained at a temperature of 283 K has shown that the fluid mass flow rate decreases with increasing the compression of the test sample. A first assessment of the stress magnitude in the test sample has been achieved by performing simplified 2-D axisymmetric structural analyses at steady state conditions using the commercial Finite Element software Ansys. For the three test runs at 283K, the comparison of the values of the permeability parameters to the corresponding magnitude of the numerically determined average compressive radial stress in the sample has shown that the permeability coefficients steadily decrease with increasing the magnitude of the compression stress. Although a 3-D FE analysis with considering the orthotropic properties of the porous material would provide more accurate results regarding the assessment of the stress magnitude, the present results demonstrate a strong and linear dependency of the permeability of the considered porous material on stress.

The results of these investigations imply that the permeability of a porous material is dependent on temperature and on stress. Although the number of the investigated test conditions (number of temperature cases and/or number of stress state cases) was limited, the fit of the permeability parameters values shows that the dependency with temperature and stress of the Darcy´s permeability *K* and Forchheimer´s permeability *G* can be cast in the following general equation

$$\begin{cases} K(T,\sigma) = aT + b\sigma + c \\ G(T,\sigma) = a'T + b'\sigma + c' \end{cases} \qquad (6)$$

where *a*, *b*, *c*, *a´*, *b´*, and *c´* are constants.

ACKNOWLEDGMENTS

This work was performed within the 'Aero-Thermodynamic Loads on Lightweight Advanced Structures II' (ATLLAS II) project investigating high-speed transport. ATLLAS II, coordinated by ESA-ESTEC, was supported by the European Union within the 7th Framework Programme theme 7 transport, contract no.: ACP0-GA-2010-263913.
Additional information related to ATLLAS II can be found on http://www.esa.int/techresources/atllas_II.

REFERENCES

[1] “Aero-Thermodynamic Loads on Lightweight Advanced Structures II ATLLAS II,” ESA, 2010.

[2] G. Cerri, A. Giovanelli, L. Battisti und R. Fedrizzi, „Advances in effusive cooling techniques of gas turbines,“ *Applied Thermal Engineering 27,* Bd. 27, pp. 692-698, 2007.

[3] E. Serbest, O. J. Haidn, D. Greuel, H. Hald und G. Korger, „Effusion cooling of throat region in rocket engines applying fiber reinforced ceramics,“ in *37th AIAA, ASME, SAE, ASEE JPC*, Salt Lake City, Utah, USA, 2001.

[4] M. Ortelt, A. Herbertz und H. Hald, „Investigations on Fibre Reinforced Combustion Chamber Structures under Effusion Cooled LOX/LH2 Operation,“ in *AIAA*.

[5] A. Gernoth, J. Riccius und D. Greuel, „Simultaneous CFD Analysis of the Hot Gas and the Coolant Flow in Effusion Cooled Combustion Chambers,“ in *IACC*, 2007.

[6] J. Riccius, A. Gernoth und D. Greuel, „Coupled CFD Analysis of the Hot Gas and the Coolant Flow in Effusion Cooled Combustion Chambers,“ in *41st AIAA/ASME/SAE/ASEE Joint Propulsion Conference & Exhibit*, 2007.

[7] W. Bouajila und R. Jörg, „A superposition methodology for modeling the multi-directional flow through a non-orthotropic porous combustion chamber wall material,“ in *Space Propulsion*, Cologne, 2014.

[8] S. Sharma und D. A. Signier, „Permeability measurement methods in porous media of fiber reinforced composites,“ *ASME Applied Mechanics Reviews,* Bd. 63, 2010.

[9] S. Abrate, „Resin flow in fiber preforms,“ *Appl Mech Rev,* Bd. 55, Nr. 6, pp. 579-599, 2002.

[10] E. Klatt, M. Kuhn und S. Hackemann, „ATLLAS_D.4.2.2_Part B Test Samples and Test Report: CMC Material Characterisation of C/C random, OXIPOL and WHIPOX for Combustors,“ ATLLAS, 2009.

[11] Hottinger Baldwin Messtechnik GmbH, *Pressure transducer P 3MA Data sheet,* 2014.

[12] Althen GmbH, „Differential Pressure Transducer AD122MK Data Sheet,“ May 2008. [Online]. Available: http://www.althensensors.com/public/media/PDF_Datenblatt/1a_Druckmesstechnik/en/A5-Z-differential-pressure-transducer-en.pdf. [Zugriff am 22 12 2014].

[13] Micro Motion und Emerson Process Management, „Product Data Sheet PS-00374, Rev. Z,“ March 2014. [Online]. Available: http://www2.emersonprocess.com/siteadmincenter/PM%20Micro%20Motion%20Documents/ELITE-PDS-PS-00374.pdf. [Zugriff am 22 12 2014].

[14] Y. Khamis und J. Riccius, „ATLLAS_D.4.2.2_Part A Flow Characterisation of CMC Samples: Tortuosity and Permeability Measurments,“ 2010.

[15] W. Bouajila und J. Riccius, „Investigation of the influence of temperature and stress on the permeability of porous continuous fiber-reinforced composite materials through experiment and simulation,“ in *6th European Conference for Aeronautics and Space Sciences (EUCASS)*, Krakow (Poland), 2015.

[16] M. A. Materials, „Copper OFHC Data Sheet,“ 2009. [Online]. Available: http://www.morganbrazealloys.com/sites/default/files/wesgo_metals_copper_ofhc.pdf. [Zugriff am 22 05 2015].